NAZARBAYEV
UNIVERSITY

CATHEPSIN G AND NEUTROPHIL ELASTASE INCREASE EXPRESSION OF MHC I ON THE CELL SURFACE OF DIFFERENT CELL LINES

MAIYA ALLAYAROVA

(B.Sc. in Biological Sciences, Nazarbayev University)

A THESIS SUBMITTED

FOR THE DEGREE OF MASTER OF LIFE SCIENCES, DEPARTMENT OF BIOLOGY,
SCHOOL OF SCIENCES AND HUMANITIES, NAZARBAYEV UNIVERSITY

2025

DECLARATION

I hereby declare that the thesis is my original work, and it has been written by me in its entirety. I have duly acknowledged all the sources of information which have been used in the thesis. This thesis has also not been submitted for any degree in any university previously.

I further declare that parts of the data and results presented in this thesis have been previously published in the journal *Molecules* (Assylbekova et al., 2024). Full publication details can be found in the reference list at the end of this document.

Maiya Allayarova

April 18, 2025

ACKNOWLEDGEMENTS

I would like to acknowledge and thank my supervisor Professor Timo Burster for his patience, help and support. His expert advice was invaluable in navigating me through this project until its completion.

I would like to express my gratitude to Akmaral Assylbekova whose help made a great contribution to my learning and positively influenced the overall direction of my work.

Last but not least, I would like to thank our group. The kindness and support of its members created an inspiring environment that fostered both my personal and professional growth.

TABLE OF CONTENTS

Nazarbayev University, School of Sciences and Humanities, Department of Biology
Master´s Degree Program in Life Sciences
Maiya Allayarova: Cathepsin G and Neutrophil Elastase Increase Expression of MHC I on the Cell Surface of Different Cell Lines.
Master of Science thesis; 32 pages, 1 appendix
Supervisor: Timo Burster, Professor, School of Sciences and Humanities, Nazarbayev University
18. 04. 2025

Keywords: MHC I, cathepsin G, neutrophil elastase

ABSTRACT

Major histocompatibility complex class I (MHC I) molecules are essential structures that enable the immune system to identify and destroy abnormal cells by presenting intracellular antigens on the cell surface. Infected or cancerous cells often escape immune recognition by downregulating MHC I molecules. Neutrophil-derived serine proteases, such as cathepsin G (CatG) and neutrophil elastase (NE), can influence MHC I expression in different cells, including peripheral blood mononuclear cells (PBMCs), glioblastoma cells, and breast cancer cells. This study examined such modulation by CatG and NE in lung cancer cell lines (A549 and H1299) and immune cells (Jurkat, T cell line). Flow cytometry analysis demonstrated that NE significantly upregulated MHC I expression in all cell types tested. In contrast, the impact of CatG was significantly more pronounced solely in Jurkat cells, implying that these cells may exhibit a more adept antigen presentation system. The apoptosis array confirmed that the observed changes in MHC I levels occur independently of cell death processes. Moreover, colorimetric substrate assay experiments showed that serum components inhibited CatG activity, suggesting that endogenous protease inhibitors may modulate its impact on antigen presentation. Together, these findings provide insights into the distinct roles of CatG and NE in increasing MHC I cell surface expression and offer potential ideas for developing therapeutic strategies aimed to improve immune recognition by generating small molecules which enhance the catalytic activity of CatG and NE.

LIST OF FIGURES AND TABLES

ABBREVIATIONS

MHC I	Major histocompatibility complex class I
CTLs	Cytotoxic T lymphocytes
ER	Endoplasmic reticulum
TAP	Transporter associated with antigen processing
NSPs	Neutrophil serine proteases
CatG	Cathepsin G
NE	Neutrophil elastase
PBMCs	Peripheral blood mononuclear cells
AAT	Alpha-1 antitrypsin
PAR1	Protease-activated receptor 1

1. INTRODUCTION

1.1 Structural features of MHC I molecule and its role in immune surveillance

The normal ability of the immune system to recognize and eliminate defective or abnormal cells relies heavily on the process of presenting intracellular antigens through major histocompatibility complex class I (MHC I) molecules, which ensures effective immune surveillance. These molecules are found on nearly all nucleated cells and are essential for activating $CD8^+$ T cells, which are also referred to as cytotoxic T lymphocytes (CTLs) (Alberts et al., 2002).

The MHC I molecule is a heterodimeric transmembrane protein consisting of a highly polymorphic α heavy chain and a non-polymorphic β_2-microglobulin. The heavy chain includes three extracellular domains α_1, α_2, and α_3, of which the α_1 and α_2 domains form the peptide-binding groove (White et al., 2014). This groove is responsible for binding peptides that are 8 to 10 amino acids long, thereby determining the specificity of antigen presentation (Li et al., 2023) (see the general structure of MHC I in Figure 1). The α_3 domain plays a critical role by interacting with the CD8 coreceptor on T cells, which is essential for T cell activation and immune response (Belyakov et al., 2007).

Structurally, the peptide-binding groove of MHC I is formed by a β-sheet platform flanked by two anti-parallel α-helices, which create several pockets that accommodate the side chains of the bound peptide. These grooves are commonly designated as A, B, C, D, E, and F. Such configuration is especially needed for determining both the affinity and specificity of peptide binding (Holland et al., 2013).

Moreover, the heavy chain of MHC I is anchored to the cell membrane via a single transmembrane domain and has a short cytoplasmic tail. The stability and surface expression of MHC I molecules depend heavily on the peptides they bind, making the peptide repertoire generated by the proteasome fundamental for effective immune surveillance (Belyakov et al., 2007).

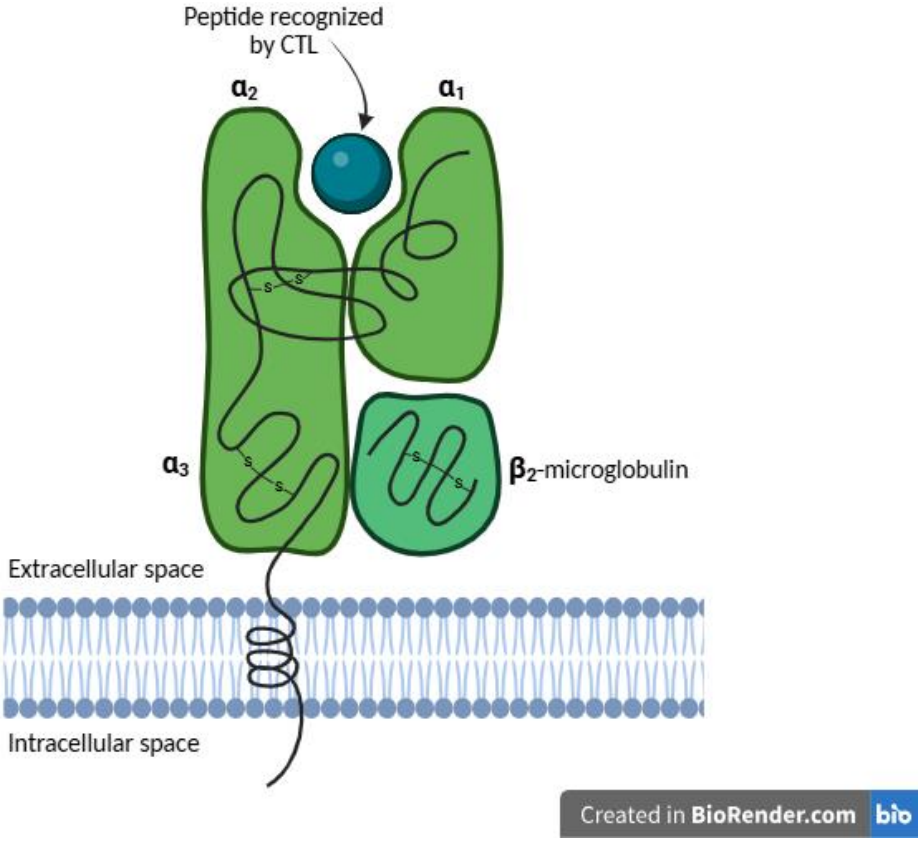

Figure 1. Structure of the MHC I molecule. (This image was created by using BioRender.com)

1.2 MHC I restricted recognition: intracellular antigen processing, MHC I presentation, and immune evasion

Intracellular proteins, including those generated by infectious pathogens or mutated genes of cancer cells (neoantigens), are constantly cleaved into peptides by the proteasome and other proteases found in the cytosol of the cell. They are then transported to the endoplasmic reticulum (ER) lumen by the transporter associated with antigen processing (TAP**)**, which not only does the transfer, but also serves as structural support for the final stages of MHC class I assembly (Hewitt, 2003). After packaging into vesicles for transport through the Golgi is completed, the complex is directed to the cell surface, where MHC I molecules present the intracellular status of the peptide repertoire on the plasma membrane, allowing $CD8^+$ T cells to monitor cells for signs of infection or malignancy (Wang et al., 2009). This immune recognition is generally detrimental to abnormal cells, as it can result in the destruction of virus-infected or transformed cells, activation of macrophages to kill intracellular bacteria, or stimulation of B cells to produce antibodies against extracellular pathogens or tumor-associated antigens. Consequently, pathogens and cancers face strong selective pressure to evade immune detection, thereby developing strategies to mitigate MHC presentation (Janeway et al., 2001).

A common strategy of tumor cells to evade immune surveillance is often characterized by the downregulation of MHC I molecules. Since $CD8^+$ T cells can only recognize antigens when such antigenic peptides are bound to MHC molecules, any reduction in MHC I expression on tumor cells can significantly impact the $CD8^+$ T cell-mediated immune response (see Figure 2). The absence of these molecules in tumors is generally linked with a poorer prognosis, as reduced MHC I expression often correlates with increased tumor growth. The immune system may even contribute to the selection of tumor cells that exhibit decreased expression of MHC I molecules (Shklovskaya et al., 2021; BNO Team, 2024). Similar mechanisms are also observed during viral infection (Braud et al., 2002). Hence, restoring or/and enhancing MHC I presentation on such cells is one of the important focuses in immunology, as it can help expose affected cells to the immune system, facilitating their clearance (Shklovskaya et al., 2021).

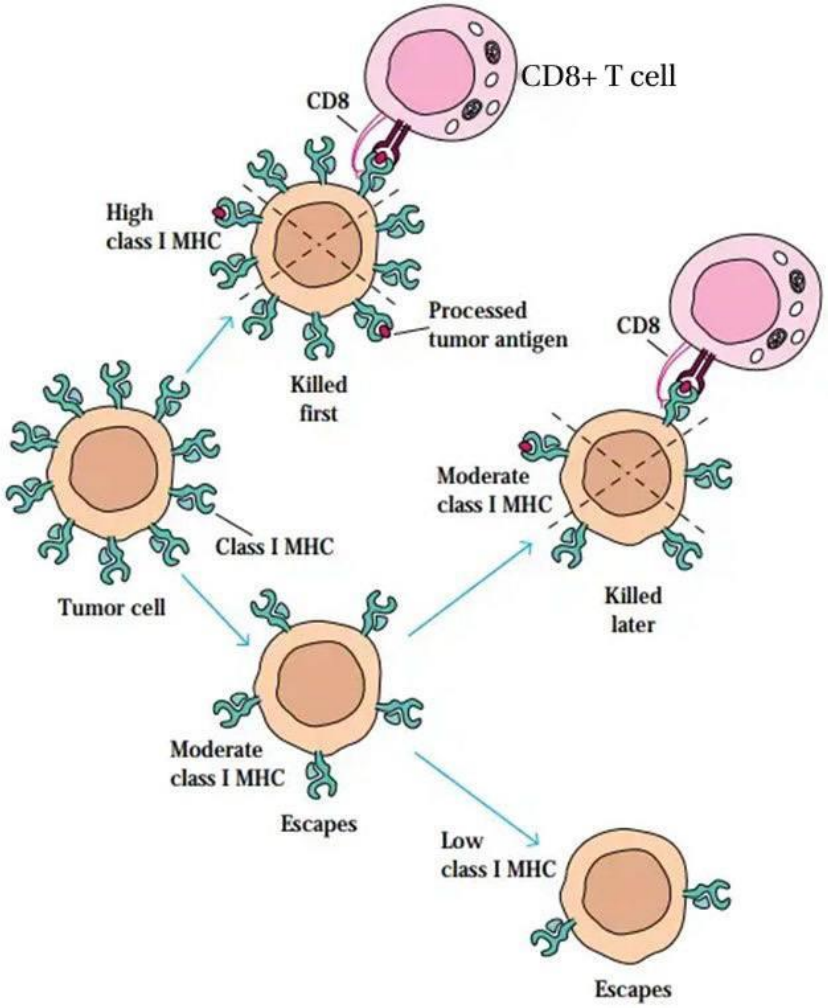

Figure 2. Downregulation of MHC I in tumor cells allows for their escape from $CD8^+$ T cells (BNO Team, 2024).

1.3 Neutrophil serine proteases and MHC I modulation

Neutrophil serine proteases (NSPs), such as cathepsin G (CatG) and neutrophil elastase (NE), are secreted by activated neutrophils in response to infections and within the tumor microenvironment. NSPs play a dual role in immune regulation, not only participating in direct pathogen destruction but also modulating immune signaling and antigen presentation (Korkmaz et al., 2010).

Previous studies showed that when exogenous CatG is introduced, it leads to an increased expression of cell surface MHC I molecules on peripheral blood mononuclear cells (PBMCs), the human acute monocytic leukemia cell line (THP-1), and human glioblastoma cells (Giese et al., 2016). Similarly, NE uptake has been shown to enhance antigen presentation and MHC I levels in breast cancer cells (Chawla et al., 2016). However, the effects of these proteases on specific lung cancer cells remain unclear.

Studying modulation of levels of MHC I molecules in the context of lung cancer is crucial since it is one of the leading causes of cancer-related deaths worldwide, mainly due to its aggressive nature and its ability to evade immune detection (Herbst et al., 2018). By investigating how CatG, NE, and their combination impact MHC I levels in lung cancer cells can provide insights into potential pathways that might restore or enhance immune recognition. Additionally, examining how Jurkat cells (which are immortalized $CD4^+$ T lymphocytes) respond to these protease treatments can help determine if they behave similarly to PBMCs (a heterogeneous population of blood cells including T cells, B cells, natural killer cells, dendritic cells, and monocytes), thus providing a useful model for immune cell responses.

1.4 Serum and tumor-derived protease inhibitors: impact on serine protease activity and MHC I immune visibility

Serum components, including protease inhibitors, may affect the activity of exogenous serine proteases. Tumor cells often secrete their own protease inhibitors (serpins) to regulate the proteolytic activity in their microenvironment (Jia et al., 2022). One example is alpha-1 antitrypsin (AAT), a protein that primarily functions as a serine protease inhibitor. AAT in its normal state effectively inhibits the activity of various enzymes, including protease 3, serine proteases like CatG and NE, acting as a protective shield against protease-driven tissue destruction (Xiang et al., 2025). Understanding this can provide valuable hints on how serum and tumor-derived factors collectively shape the immune visibility of cancer cells, thus offering potential for therapeutic intervention aimed at restoring or enhancing MHC I presentation.

2. MATERIALS AND METHODS

2.1 Cell culture

This study used several cell lines, including human adenocarcinoma alveolar basal epithelial cells (A549; CCL-185, American Type Culture Collection, ATCC, Manassas, VA, USA), human epithelial like non-small cell lung carcinoma cells derived from the lymph node (NCI-H1299, abbreviated H1299; CRL-5803, American Type Culture Collection, ATCC, Manassas, VA, USA), and human T cell lymphoblasts (Jurkat E6-1 cells, abbreviated Jurkat; ARP-177, BEI Resources, NIAID, NIH, Bethesda, MD, USA). All cell lines were grown in RPMI-1640 (R8755-1L, Lot No. SLBF1516V, Sigma-Aldrich, St. Louis, MO, USA) medium supplemented with 10% Fetal Bovine Serum (FBS, Lot No. 2631713RP, Gibco, Grand Island, NY, USA), which was inactivated by heat at 56°C for 30 min, and 1% Penicillin–Streptomycin (pen-strep, Lot No. 210496, Gibco, Grand Island, NY, USA).

Adherent cells (A549, H1299) were cultured in T25, T75 flasks or 10 cm dishes until 85–90% confluency. Their growth was monitored every 3 days, and the media from the flasks or plates were aspirated, and cells were washed using PBS (room temperature, RT) pH 7.4 (Lot No. RNBL5991, Sigma-Aldrich, St. Louis, MO, USA). Cells were detached by adding 1 to 5 ml of 1X Trypsin-EDTA (Lot No. 2537762, Gibco, Grand Island, NY, USA) and incubated at 37°C for 3–7 minutes until detachment occurred. Trypsin was then inactivated with two volumes of pre-warmed complete RPMI-1640 before centrifugation (250×g, 5 min, RT). Jurkat suspension cells were maintained in T25 and T75 flasks and passaged every 3 days at 5×10^5 cells/ml (not exceeding 2×10^6 cells/ml), and then centrifuged at 200×g for 5 min (RT). All cells were counted and plated according to the requirements of the experiment.

2.2 Apoptosis profiling via Proteome Profiler Human Apoptosis Array Kit

Cell treatment: Jurkat cells were seeded in T25 flasks at the final amounts of 6×10^6 to 7×10^6 cells per sample. Cells were treated in serum-free RPMI-1640 for 4 hours as follows: control, CatG (Cathepsin G, Human Neutrophil, PN: 16-14-030107, Lot No. CG2023-01, Athens Research & Technology, Athens, GA, USA) final concentration of 10 µg/ml [10 µg/ml], NE (Elastase, Human Neutrophil, PN: 16-14-051200, Lot No. EH2022-01, Athens Research & Technology, Athens, GA, USA) [10 µg/ml], and CatG [10 µg/ml] + NE [10 µg/ml]. After incubation, cells were collected, transferred to 15ml Eppendorf tubes, and centrifuged at 200×g for 5 min. The supernatant from each tube was aspirated and cells were washed twice with 5ml

PBS each. Any remaining PBS was aspirated to produce so-called dry pellet. Cell lysates were then prepared.

Proteome Profiler Human Apoptosis Array Kit: According to the company's protocol (Human Apoptosis Array, Lot No. 1718009, R&D Systems, Minneapolis, USA), after the treatment, Jurkat cells were lysed using Lysis Buffer 17. The protein concentration for each sample was quantified by a Bradford assay (Bio-Rad Laboratories). The Proteome Profiler Array membrane was first equilibrated and blocked by using 2 ml of Array Buffer 6 in a 4-well dish for 1 h at RT. During this blocking step on the shaker, 0.4 mg of Jurkat cell lysate was mixed with Array Buffer 6 to a final volume of 1.5 ml to which protease inhibitors leupeptin (Catalog No. 1167, Tocris Bioscience, UK), aprotinin (Catalog No. 4139, Tocris Bioscience, UK), and pepstatin A (Catalog No. 1190, Tocris Bioscience, UK) at a final concentration of 10 µM were added, and incubated for 1 h at RT. All samples were on the shaker during this process. After aspirating the Array Buffer 6 from the dish, the sample was added to the corresponding membranes and incubated overnight at 4°C on a shaker. Following the next day, the membranes were washed for 10 min three times and were incubated with 15 µl of the Apoptosis Detection Antibody Cocktail in 1.5 ml Array Buffer 6, and incubated for 1 h at RT on a shaker. After additional 3 washing steps, 1:2000 Streptavidin-HRP solution in Array Buffer 6 (2 ml) was added to the membrane for 30 min at RT on a shaker. Three more washes were done after this step, and 1 ml of Chemi Reagent Mix was used to develop the membrane. The chemiluminescence was visualized using a ChemiDoc MP detector (Bio-Rad), and analyzed in Image Lab Touch Software (Bio-Rad).

2.3 Flow cytometry analysis of cell surface MHC I levels after protease treatments

A549, H1299, and Jurkat cells were seeded into 24-well plate in complete medium (RPMI-1640, 10% FBS, 1% pen-strep) a day before treatment. Adherent cells were seeded at a confluency of 1.0×10^5 to 1.2×10^5 cells/well, and suspension cells were at a confluency of 2×10^5 cells/well. On the next day, cells were incubated with the proteases: CatG [10 µg/ml], NE [10 µg/ml], or their combination (CatG [10 µg/ml] + NE [10 µg/ml]) for 6 h in PBS at 37°C in the incubator with 5% CO_2. After 6 hours, adherent cells A549 and H1299 were detached using trypsin, and the pellets were washed with 5 ml of PBS pH 7.4 each, while Jurkat cell suspensions were directly washed with PBS. Then, all cell pellets were transferred to Eppendorf tubes (1.5 ml) and washed with 250 µl of FACS buffer (PBS pH 7.4 + 1% FBS) for each sample. Cells were stained with an anti-human HLA-ABC monoclonal antibody conjugated with APC (W6/32, Lot No. 4289568, eBioscience by Thermo Fisher Scientific,

Waltham, MA, USA). For each cell line, both an untreated control (cells that were not exposed to proteases, incubated in PBS for 6 h, and stained with the anti-human HLA-ABC antibody) and an isotype control (untreated cells incubated in PBS for 6 h and stained with mouse IgG2a kappa (eBM2a) conjugated to APC (Lot No. 4289571, eBioscience, Waltham, MA, USA)) were included. The antibody was added (0.5 µl in 100 µl of FACS buffer per sample) and incubated on ice for 30 min. Following incubation, the pellets were washed twice with 250 µl of FACS buffer for 5 min each. Finally, all samples were analyzed on an Attune Nxt Flow Cytometer (Thermo Fisher Scientific, Waltham, MA, USA), with cell populations gated and the median fluorescence intensity (MFI) in the RL1-A channel recorded.

2.4 Microplate-based spectrophotometric assay of Suc-VPF-pNA degradation by CatG

The colorimetric substrate succinyl-L-Val-Pro-Phe-p-nitroanilide (Suc-VPF-pNA), which is a colorimetric substrate for CatG, was used (refer to chemical structure on Figure 3) (Zou et al., 2012). CatG preferentially cleaves after phenylalanine, releasing the p-nitroanilide group and producing a characteristic yellow color detectable by spectrophotometry. CatG was added under three different conditions: complete medium (RPMI-1640, 10% FBS, 1% pen-strep), serum-free medium (RPMI-1640, 1% pen-strep), and 1X PBS (pH 7.4). The Suc-VPF-pNA substrate was then added to each well at a final concentration of 200 µM with $MgCl_2$ [0.1 M] solution, and measurements were taken using a 96-well plate reader (Varioskan Flash Multimode Reader, Thermo Fisher Scientific) at 405 nm every 15 minutes for a total of 1 h. Substrate turnover values were recorded and compared across all conditions. Additional experiments were conducted to confirm the specificity of CatG and substrate turnover levels, where a Cathepsin G inhibitor I (CatG inhibitor, Cayman Chemical Company, Michigan, USA) was used. Two master mixes (MM) were prepared: one containing the substrate Suc-VPF-pNA [200 µM] and the other containing the CatG inhibitor [20 µM]. Both contained $MgCl_2$ at the final concentration of 0.1 M. They were prepared in three different conditions as before. The MM with inhibitor was added to the plate first, followed by CatG (starting at [5 µg/ml] and titrated down) to the designated wells, and finally the substrate MM was added to all wells. Measurements were taken using the same Varioskan plate reader at 405 nm every 15 minutes over a 1 h period.

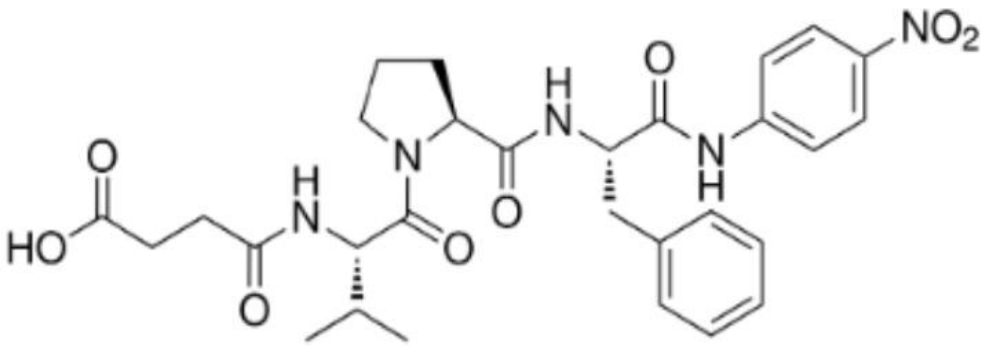

Figure 3. Chemical structure of Suc-VPF-pNA, a colorimetric substrate specific to CatG (Eipper et al., 2016).

2.5 Flow cytometry analysis of serum-induced modulation of MHC I cell surface expression

Jurkat cells were seeded into 24-well plates in complete RPMI-1640 medium at a density of 2×10^5 cells per well and incubated overnight. The following day, cells were exposed to three different environments: complete medium (RPMI-1640, 10% FBS, 1% pen-strep), serum-free medium (RPMI-1640, 1% pen-strep), and 1X PBS of pH 7.4. Simultaneously, cells in each condition were treated with CatG [10 µg/ml] for 6 h at 37 °C. For each environment, untreated controls (cells without protease treatment) were included. After incubation, cells were washed twice with 5 ml of PBS. Cells were stained as previously described in section 2.3 with an anti-human HLA-ABC monoclonal antibody (W6/32) conjugated with APC (eBioscience). An isotype control was also included, consisting of untreated cells stained with mouse IgG2a kappa (eBM2a) conjugated to APC (eBioscience). Flow cytometry analysis was performed using an Attune Nxt Flow Cytometer (Thermo Fisher Scientific), followed by the description outlined in section 2.3.

2.6 Data analysis

Raw data from flow cytometry were analyzed in FlowJo v10.8.1 software for gating and obtaining median fluorescent intensity values. All data produced in this research were analyzed using GraphPad Prism 10.2.3 software for statistical significance determination and graphical representation. Appropriate statistical tests were applied to determine significance and indicated in the figure legend.

3. AIMS OF THE THESIS PROJECT

The primary hypothesis of this study is that exogenous administration of serine proteases CatG and NE enhances the surface expression of class I MHC molecules on lung cancer (A549, H1299) and immune (Jurkat) cells.

A secondary hypothesis is that serum components in the medium applied to cells may modulate the activity of CatG and subsequently influence MHC I expression levels.

To test these hypotheses, the following aims should be achieved:

Aim 1. Evaluate the effect of CatG and NE treatment on the expression of MHC I molecules on the surface of different cell lines *in vitro*.

Objectives:

- Perform apoptosis profiling using a human apoptosis array to determine whether any apoptotic markers change their expression following protease treatment.
- Treat cells with CatG, NE, or a combination of both for 6 hours and measure MHC I expression levels using flow cytometry.
- Determine and statistically analyze the potential additive effect of CatG and NE on MHC I levels, comparing single treatments with combinations across A549, H1299, and Jurkat cells.

Aim 2. Assess the impact of serum on the levels of MHC I molecules on the cell surfaces of Jurkat cells.

Objectives:

- Measure the activity of CatG to degrade Suc-VPF-pNA substrate under different conditions (medium + 10% FBS, medium + 0% FBS, 1X PBS) by spectrophotometry.
- Treat cells with CatG for 6 hours in different conditions (medium + 10% FBS, medium + 0% FBS, 1X PBS) and measure MHC I surface levels using flow cytometry.

4. RESULTS

4.1 The expression of key markers of apoptosis is not altered by CatG, NE, or their combination during short-term exposure in Jurkat cells

The apoptosis profiler array was utilized to identify apoptosis in Jurkat cells that were either untreated or treated with CatG [10 µg/ml], NE [10 µg/ml], or a combination of both CatG and NE at the same concentration. Cell lysate samples of Jurkat cells showed no change in expression of key apoptosis markers, including cleaved caspase-3 and survivin (see Figure 4). Thus, exposure to CatG, NE, or their combination does not activate apoptotic pathways in Jurkat cells, meaning that any subsequent changes in MHC I expression occur independently of apoptosis. The list of complete apoptosis markers is demonstrated in Table A 1.

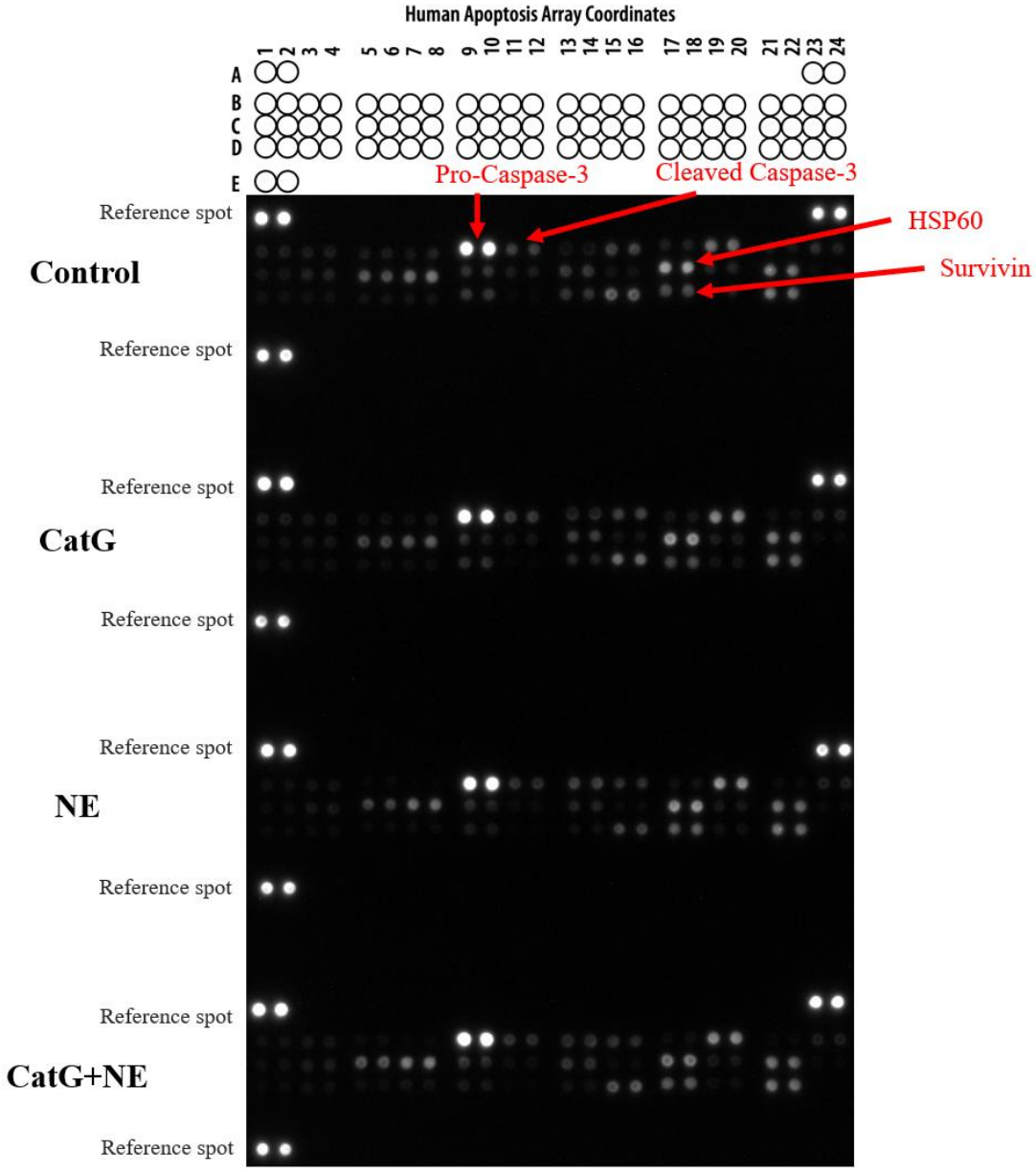

Figure 4. The apoptosis profiler array was applied to detect different apoptosis markers in Jurkat cells untreated and treated with CatG [10 µg/ml], NE [10 µg/ml], or the combination of CatG [10 µg/ml] and NE [10 µg/ml].

4.2 CatG and NE induce upregulation of MHC I on the cell surface of A549, H1299, and Jurkat cells

A549, H1299, and Jurkat cells were incubated with CatG [10 µg/ml], NE [10 µg/ml], and their combination (CatG [10 µg/ml] and NE [10 µg/ml]) for 6 hours in PBS. Treatments with CatG, NE, and the combination of CatG and NE showed varying results for A549, H1299 and Jurkat cell lines in terms of MHC I upregulation. For A549 and H1299 cells, CatG did not significantly increase MHC I surface expression, while treatment with NE did. The protease combination further enhanced the upregulation of MHC I, showing a slight additive effect, but not significantly more compared to when only NE was used. In comparison to Jurkat cells, both CatG or NE significantly induced upregulation of MHC I (refer to Figure 5).

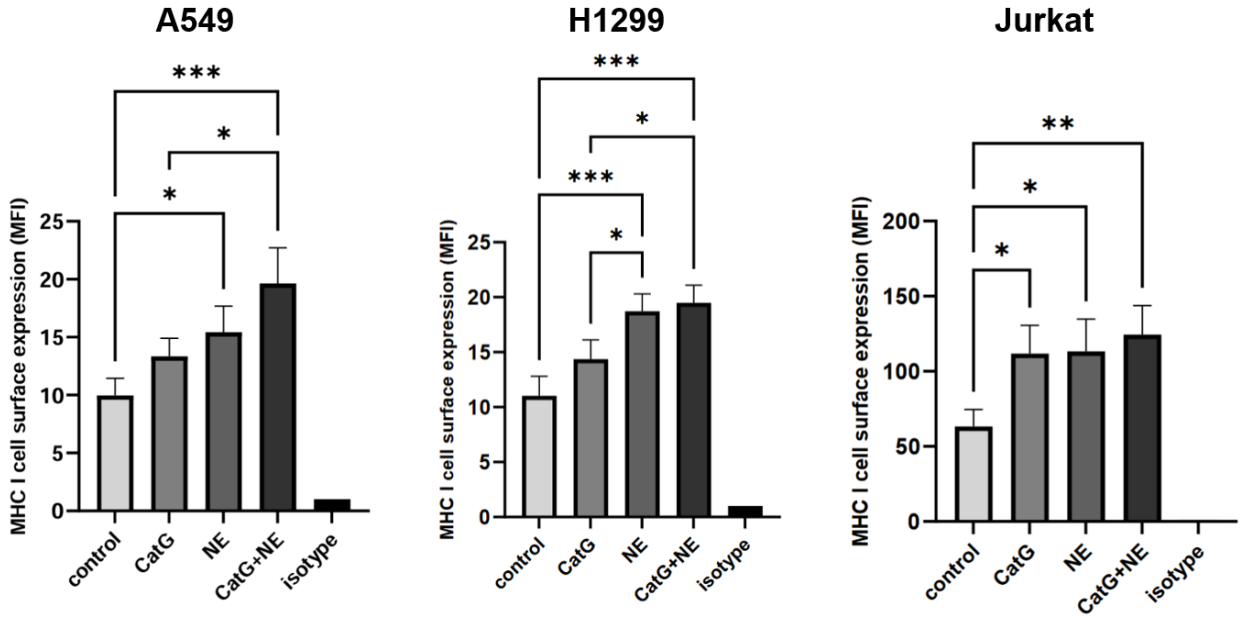

Figure 5. Flow cytometric assessment of MHC I cell surface expression after treatment of A549, H1299, and Jurkat cells with CatG [10 µg/ml], NE [10 µg/ml], or both for 6h in PBS. All values of data were normalized to isotype controls and considered significant at $p \leq 0.05$ (*), $p \leq 0.01$ (**), or $p \leq 0.001$ (***) by using an unpaired one-way ANOVA and Sidak post hoc test, n = 3. The *y-axis* represents median fluorescent intensity (MFI) in arbitrary units (AU), the *x-axis* denotes the names of samples: control (untreated), CatG, NE, CatG + NE, and isotype.

4.3 The proteolytic turnover of the Suc-VPF-pNA substrate by CatG is inhibited by serum components in the medium

The turnover of the colorimetric substrate Suc-VPF-pNA by different concentrations of CatG was tested under three different conditions: complete medium (RPMI-1640 with 10% FBS), serum-free medium (RPMI-1640 with 0% FBS), and PBS (pH 7.4). CatG digested the substrate Suc-VPF-pNA in a dose- and environment-dependent manner, and this activity was effectively blocked by the CatG inhibitor (Figure 6).

Figure 6 (A-F, panel i) shows that Suc-VPF-pNA cleavage was increased depending on incubation time for all tested CatG concentrations, with the most prominent activity observed in PBS condition. The presence of serum (10% FBS) generally reduced proteolytic activity, and for serum-free medium (0% FBS), more noticeably at lower CatG concentrations. When CatG inhibitor [20 μM] was added (Figure 6, A-F, panels ii), it almost completely suppressed substrate degradation in all conditions, confirming CatG-specificity. As for panels iii, at CatG [5 μg/ml] (Figure 6 A), no significant differences were found between PBS and media conditions, likely due to CatG overruling the inhibitory effects of serum. At CatG [2.5 μg/ml] (Figure 6 B), a considerable difference was observed only at the 15-minute time point between PBS and 10% FBS, indicating early CatG inhibition by serum. At 1.25 μg/ml (Figure 6 C) and 0.63 μg/ml (Figure 6 D), there were significant reductions in activity in 10% FBS compared to PBS at 30, 45, and 60 minutes, showing a clear serum-mediated inhibition at moderate CatG concentrations. When comparing PBS vs. 10% FBS in other concentrations of CatG, for instance, 0.31 μg/ml (Figure 6 E) and 0.16 μg/ml (Figure 6 F)), significant differences were observed at 45 and 60 minutes. PBS compared to 0% FBS at these concentrations showed a considerable difference in substrate turnover by CatG only at 60 minutes incubation, indicating that even in serum-free media, some inhibitory effect may still occur; however, delayed. Hence, CatG-mediated substrate turnover is progressively inhibited by serum components in a concentration- and time-dependent manner.

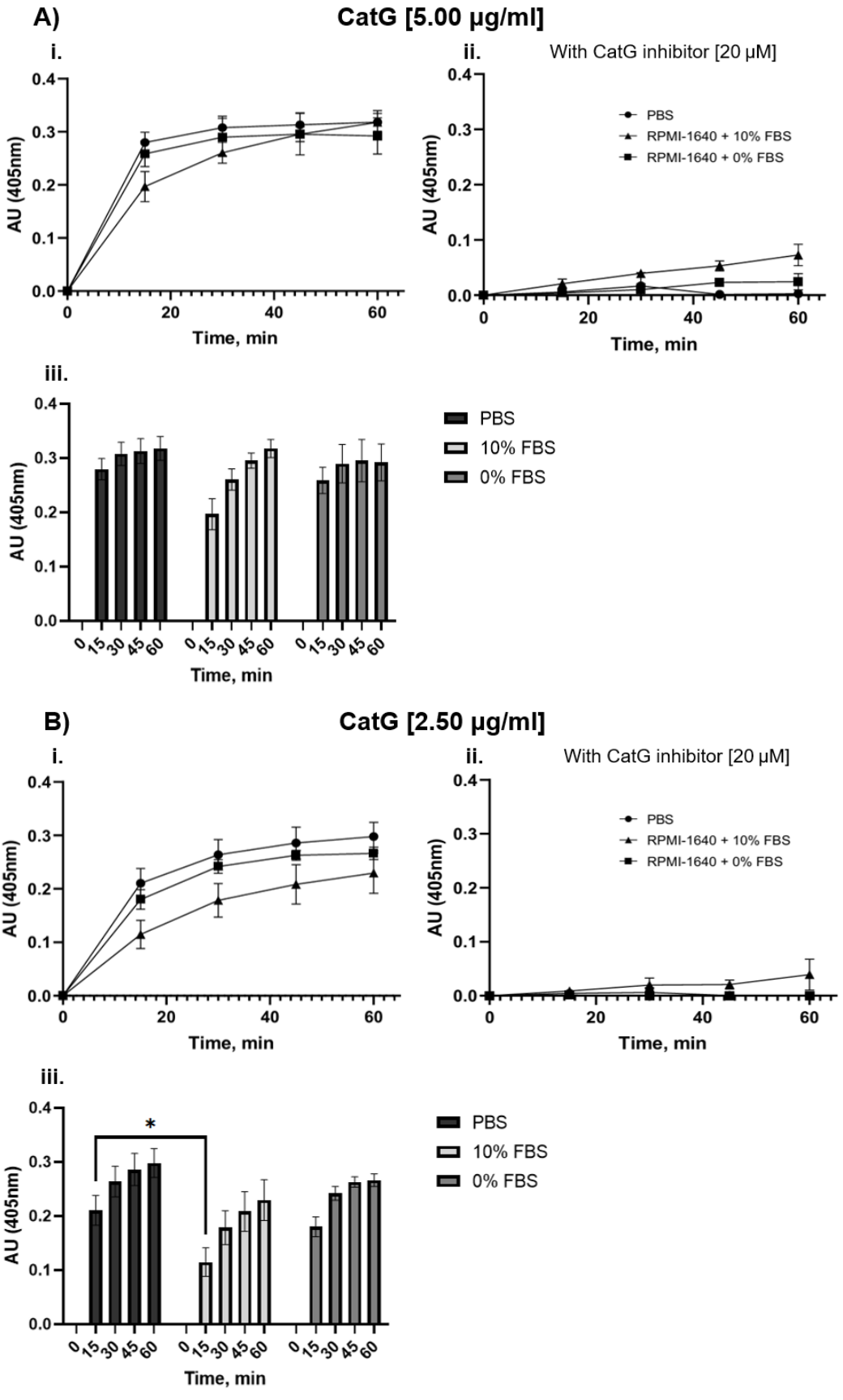
A)
CatG [5.00 µg/ml]
i.
ii.
With CatG inhibitor [20 µM]
AU (405nm)
Time, min
PBS
RPMI-1640 + 10% FBS
RPMI-1640 + 0% FBS
iii.
PBS
10% FBS
0% FBS
B)
CatG [2.50 µg/ml]
i.
ii.
With CatG inhibitor [20 µM]
iii.
*

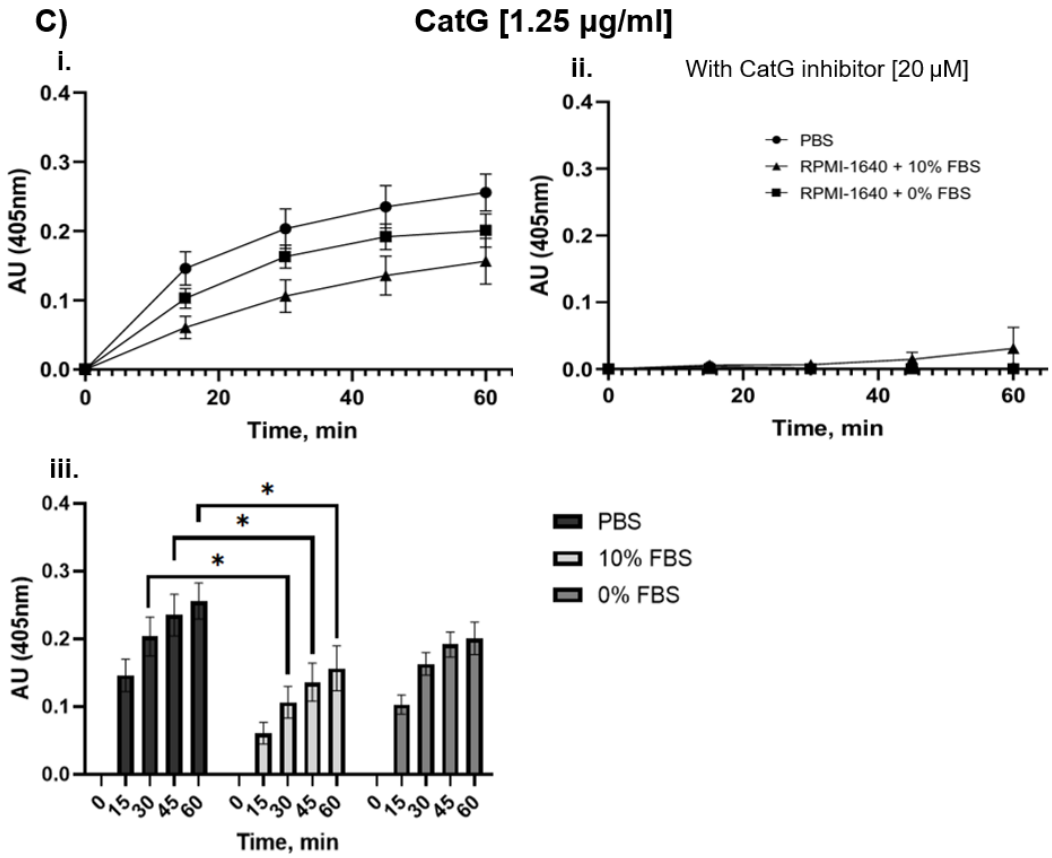
C)
CatG [1.25 µg/ml]
i.
ii.
With CatG inhibitor [20 µM]
AU (405nm)
Time, min
PBS
RPMI-1640 + 10% FBS
RPMI-1640 + 0% FBS
iii.
PBS
10% FBS
0% FBS

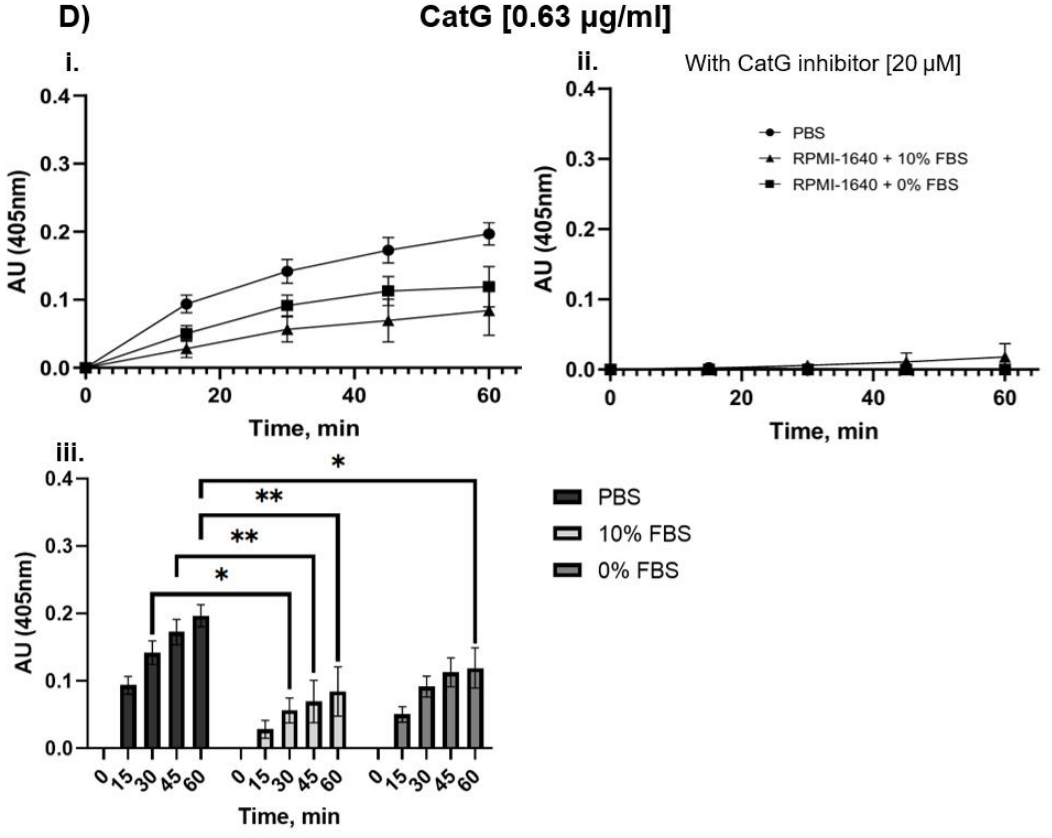
D)
CatG [0.63 µg/ml]
i.
ii.
With CatG inhibitor [20 µM]
AU (405nm)
Time, min
PBS
RPMI-1640 + 10% FBS
RPMI-1640 + 0% FBS
iii.
PBS
10% FBS
0% FBS

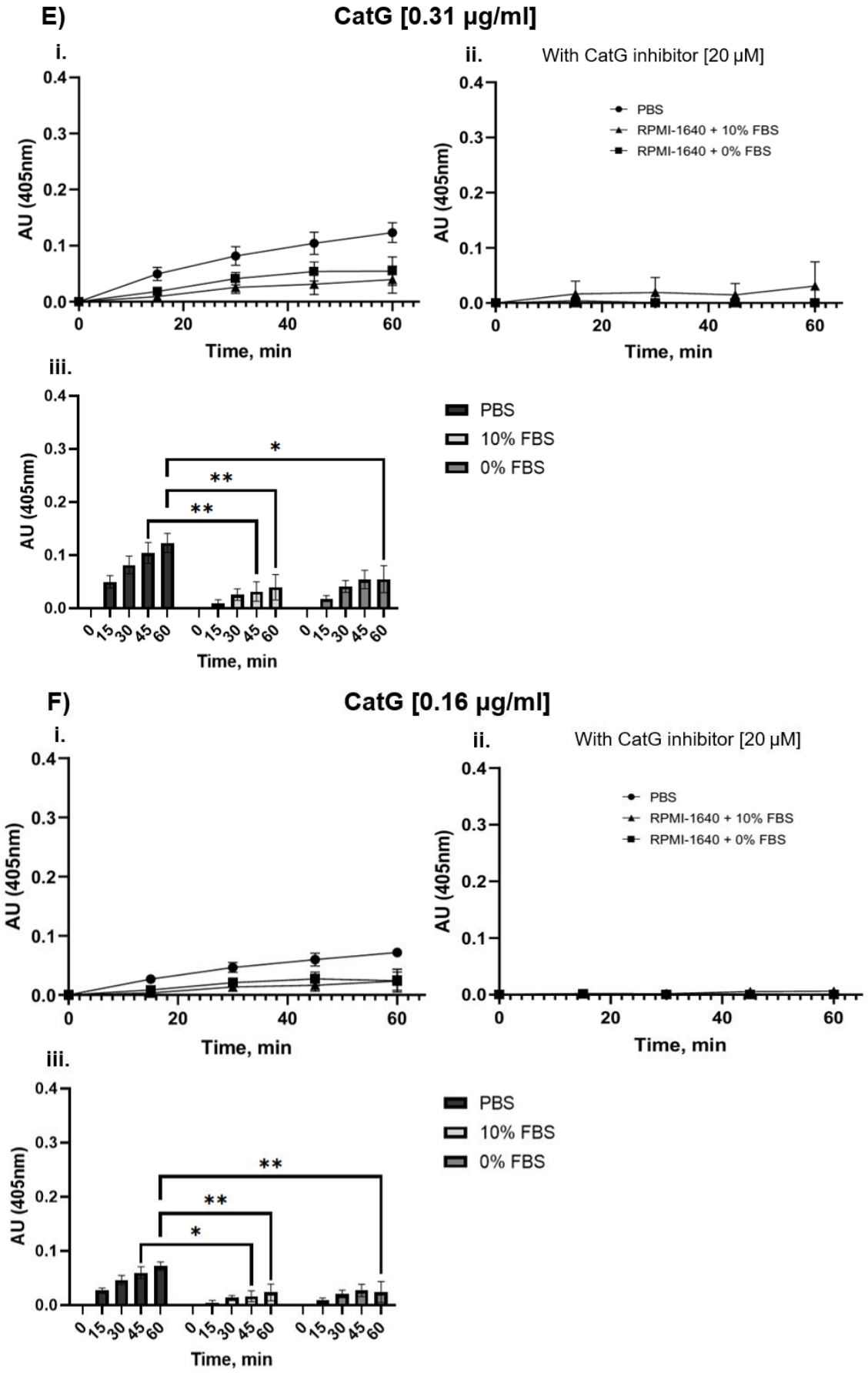
E)
CatG [0.31 µg/ml]
i.
ii.
With CatG inhibitor [20 µM]
PBS
RPMI-1640 + 10% FBS
RPMI-1640 + 0% FBS
AU (405nm)
Time, min
iii.
PBS
10% FBS
0% FBS
*
**
**
F)
CatG [0.16 µg/ml]
i.
ii.
With CatG inhibitor [20 µM]
PBS
RPMI-1640 + 10% FBS
RPMI-1640 + 0% FBS
AU (405nm)
Time, min
iii.
PBS
10% FBS
0% FBS
**
**
*

Figure 6. Dose-dependent proteolytic activity of CatG and its inhibition in the presence or absence of serum. Different concentrations of CatG were used: **A)** CatG [5 µg/ml], **B)** CatG [2.5 µg/ml], **C)** CatG [1.25 µg/ml], **D)** CatG [0.63 µg/ml], **E)** CatG [0.31 µg/ml], and **F)** CatG [0.16 µg/ml]. The numeration i signifies – a graph for the degradation of Suc-VPF-pNA [200 µM] by CatG in three types of environments: PBS; complete RPMI-1640 (10% FBS); serum-free RPMI-1640 (0% FBS); ii – degradation of substrate when samples were treated with CatG inhibitor [20 µM]; iii – bar diagrams with significant levels for i. Blank values were subtracted from all values and significance was considered at $p \leq 0.05$ (*) or $p \leq 0.01$ (**) by using two-way ANOVA and Tukey's multiple comparisons test, n = 2. The *y-axis* represents spectrophotometric measurements at 405nm in arbitrary units (AU), the *x-axis* denotes the time of incubation.

4.4 Serum components inhibit CatG activity thereby preventing MHC I upregulation in Jurkat cells

Based on the flow cytometry experiment data, CatG significantly increased MHC I surface expression in both 0% FBS and PBS conditions, while no significant change was observed in medium containing 10% FBS, suggesting that serum components inhibited the proteolytic activity of proteases and diminished the effect of MHC I upregulation (Figure 7 A). Among CatG-treated cells, MHC I expression was significantly higher in 0% FBS and PBS compared to 10% FBS, again highlighting that serum suppresses the effect of CatG. The expression levels in PBS and 0% FBS are similar. In conclusion, the absence of serum allows CatG to effectively enhance MHC I surface levels (Figure 7 B).

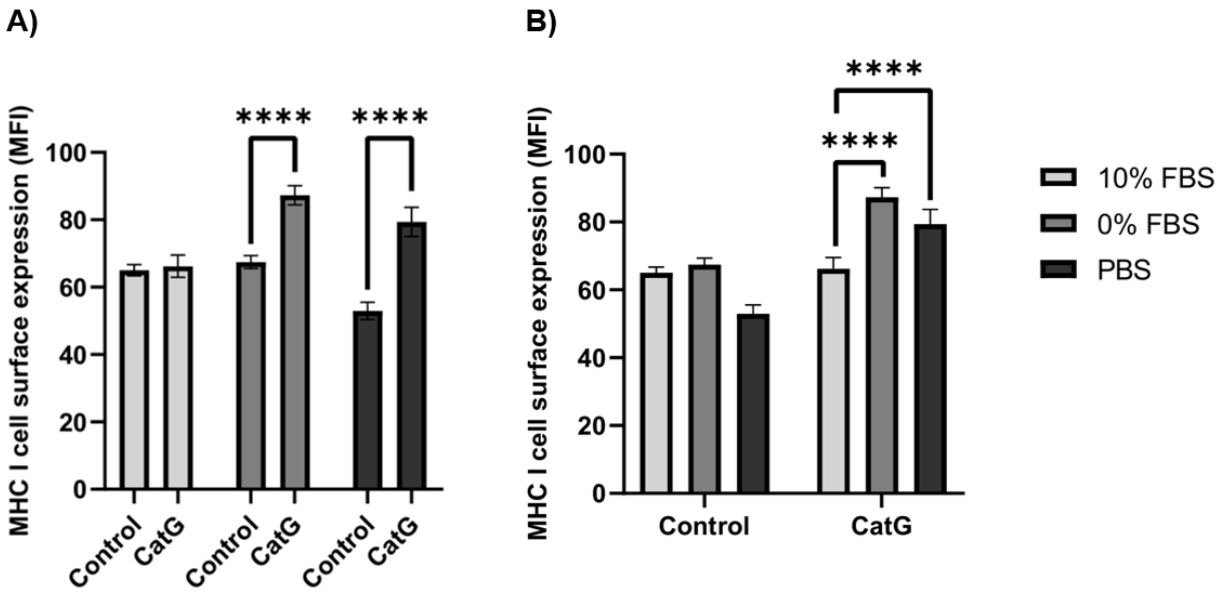

Figure 7. Flow cytometry assessment of MHC I cell surface expression after treatment of Jurkat cells with CatG. CatG [10 µg/ml] under different conditions, such as complete RPMI-1640 (10% FBS), serum-free RPMI-1640 (0% FBS), or PBS: **A)** comparison of MHC I expression within each specific condition (control vs. CatG treated); **B)** comparison of CatG-treated groups under different conditions (10% FBS, 0% FBS, or PBS). All values were normalized to the isotype control and considered significant at $p \leq 0.0001$ (****) by using two-way ANOVA and Tukey's multiple comparisons test, n = 4. The *y-axis* represents median fluorescent intensity (MFI) in arbitrary units (AU), the *x-axis* denotes the names of samples: control (untreated cells) and CatG.

5. DISCUSSION

This study investigated whether exogenous administration of CatG and NE would enhance the surface expression of MHC I molecules on A549, H1299, and Jurkat cells and assessed the modulatory role of serum components on CatG activity.

As the results showed, treatment with CatG, NE, and their combination did not trigger apoptosis in Jurkat cells, as confirmed by the human apoptosis array (Figure 4). Expression of markers, such as cleaved caspase-3, survivin, HSP60, and others (Table A 1) was not changed, ensuring that any observed changes in MHC I surface expression are independent of apoptosis-induced effects. Similar results were also observed by our group for A549 and H1299 cells (Assylbekova et al., 2024).

Flow cytometry data indicated that both CatG and NE independently enhance MHC I cell surface expression depending on the cells analyzed (refer to Figure 8). For lung cancer cells, only NE treatment provoked a significant upregulation effect, while the levels of MHC I molecules on Jurkat cells were increased further by both CatG and NE compared with the levels of MHC I observed on A549 or H1299 cells (Figure 5). The different response of cells to the proteases could be attributed to their distinct cellular entry and signaling pathways. When NE enters the cell via clathrin pit-mediated endocytosis (Gregory et al., 2012), it supports the stabilization and increase in cell surface MHC I molecules by decreasing their turnover, thereby enhancing immunogenic antigen presentation by MHC I (Peters et al., 2017). As for CatG, it is proposed to upregulate MHC I via the cell surface protease-activated receptor 1 (PAR1) by increasing the recycling process of MHC I back to the cell surface (Giese et al., 2016; Burster et al., 2020). These distinct mechanisms may explain why CatG and NE have a more noticeable effect on MHC I expression in Jurkat cells compared to lung cancer cells. In context, the enhanced upregulation of MHC I in immune cells suggests that these cells may have intrinsic differences in antigen presentation machinery, requiring heightened surveillance for infection to prevent the dissemination of viruses.

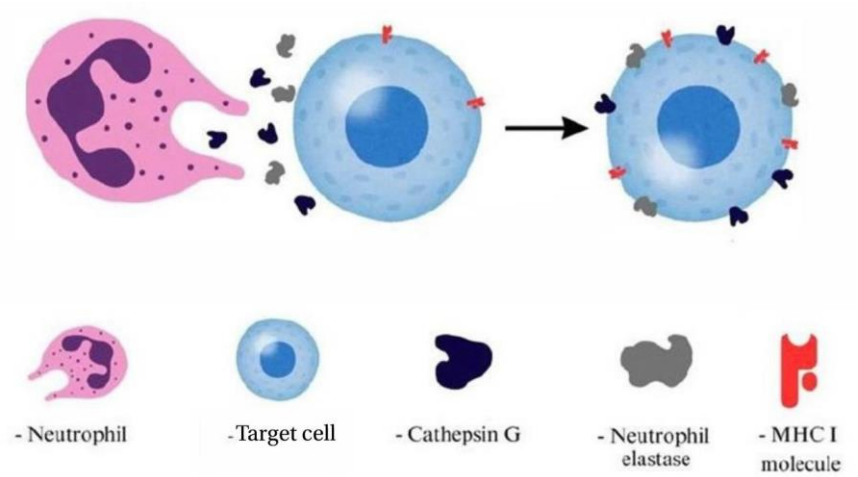

Figure 8. A proposed response of the cell after treatment with CatG or/and NE (Assylbekova et al., 2024).

Another aspect that this study found is the significant influence of serum components on CatG activity and, consequently, on MHC I cell surface expression. Experiments using Suc-VPF-pNA demonstrated that CatG-mediated substrate turnover was dose-dependent and was most effective in PBS; however, CatG activity gradually declined in serum-free (0% FBS) and especially under serum-containing conditions (10% FBS; see Figure 6). This inhibition could be explained by the presence of protease inhibitors like serpins, thereby limiting CatG's capacity to modulate levels of MHC I at the cell surface. Flow cytometry data confirmed this observation further. Upon treatment of Jurkat cells with CatG in PBS or serum-free medium, MHC I surface expression increases significantly compared to cells in complete medium (refer to Figure 7). It could mean that serum-derived factors from FBS interfere with the proteolytic activity of CatG, thereby reducing its impact on MHC I upregulation. From a physiological point of view, such inhibition may help avoid excessive proteolytic damage to host tissues but could also impair the beneficial immunomodulatory effects of proteases during immune defense (Xiang et al., 2025).

A potential limitation of this study is that only immortalized cell lines were used under short-term exposure conditions, which may not fully reflect the complexity of *in vivo* tumor or inflammatory microenvironments. Therefore, future work will extend these findings to primary patient-derived cells and appropriate animal models to validate the relevance of CatG- and NE-mediated MHC I modulation *in vivo*.

6. CONCLUSION

In summary, this study showed that exogenous administration of CatG and NE enhances MHC I cell surface expression in both lung cancer and immune cells, with NE significantly upregulating MHC I in all cell types and CatG having an effect mainly on Jurkat cells. The lack of changes in apoptotic markers confirms that these effects are independent of cell death. Furthermore, the inhibitory influence of serum on CatG activity, and consequently on MHC I upregulation, demonstrates the complexity of the inflammation or tumor microenvironment, where endogenous protease inhibitors or other serum-derived factors can modulate protease-driven antigen presentation.

7. REFERENCES

Alberts, B., Johnson, A., Lewis, J., Raff, M., Roberts, K., & Walter, P. (2002). *Molecular biology of the cell* (4th ed.). Garland Science. https://www.ncbi.nlm.nih.gov/books/NBK26926/

Assylbekova, A., Allayarova, M., Konysbekova, M., Bekturgan, A., Makhanova, A., Brown, S., Grzegorzek, N., Kalbacher, H., Kalendar, R., & Burster, T. (2024). The proteolytic activity of neutrophil-derived serine proteases bound to the cell surface arming lung epithelial cells for viral defense. *Molecules, 29*(18), 4449. https://doi.org/10.3390/molecules29184449

Belyakov, I. M., Kozlowski, S., Mage, M., Ahlers, J. D., Boyd, L. F., Margulies, D. H., & Berzofsky, J. A. (2007). Role of alpha3 domain of class I MHC molecules in the activation of high- and low-avidity CD8+ CTLs. *International immunology*, *19*(12), 1413–1420. https://doi.org/10.1093/intimm/dxm111

BNO Team. (2024, April 10). Tumor Antigen. *Biology Notes Online.* Retrieved November 7, 2024, from https://biologynotesonline.com/tumor-antigen/

Braud, V. M., Tomasec, P., & Wilkinson, G. W. (2002). Viral evasion of natural killer cells during human cytomegalovirus infection. *Current Topics in Microbiology and Immunology, 269,* 117–129. https://doi.org/10.1007/978-3-642-59421-2_8

Burster, T., Knippschild, U., Molnár, F., & Zhanapiya, A. (2020). Cathepsin G and its dichotomous role in modulating levels of MHC class I molecules. *Archivum Immunologiae et Therapiae Experimentalis, 68*(4), 25. https://doi.org/10.1007/s00005-020-00585-3

Chawla, A., Alatrash, G., Philips, A. V., Qiao, N., Sukhumalchandra, P., Kerros, C., Diaconu, I., Gall, V., Neal, S., Peters, H. L., Clise-Dwyer, K., Molldrem, J. J., & Mittendorf, E. A. (2016). Neutrophil elastase enhances antigen presentation by upregulating human leukocyte antigen class I expression on tumor cells. *Cancer Immunology, Immunotherapy: CII, 65*(6), 741–751. https://doi.org/10.1007/s00262-016-1841-6

Giese, M., Turiello, N., Molenda, N., Palesch, D., Meid, A., Schroeder, R., Basilico, P., Benarafa, C., Halatsch, M. E., Zimecki, M., & others. (2016). Exogenous cathepsin G upregulates cell surface MHC class I molecules on immune and glioblastoma cells. *Oncotarget, 7*(46), 74602–74611. https://doi.org/10.18632/oncotarget.12980

Gregory, A. D., Hale, P., Perlmutter, D. H., & Houghton, A. M. (2012). Clathrin pit-mediated endocytosis of neutrophil elastase and cathepsin G by cancer cells. *The Journal of Biological Chemistry*, *287*(42), 35341–35350. https://doi.org/10.1074/jbc.M112.385617

Herbst, R. S., Morgensztern, D., & Boshoff, C. (2018). The biology and management of non-small cell lung cancer. *Nature, 553*(7689), 446–454. https://doi.org/10.1038/nature25183

Hewitt, E. W. (2003). The MHC class I antigen presentation pathway: Strategies for viral immune evasion. *Immunology, 110*(2), 163–169. https://doi.org/10.1046/j.1365-2567.2003.01738.x

Holland, C. J., Cole, D. K., & Godkin, A. (2013). Re-directing CD4(+) T cell responses with the flanking residues of MHC class II-bound peptides: The core is not enough. *Frontiers in Immunology, 4*, 172. https://doi.org/10.3389/fimmu.2013.00172

Janeway, C. A., Jr., Travers, P., Walport, M., & Shlomchik, M. (2001). *Immunobiology: The immune system in health and disease* (5th ed.). Garland Science. https://www.ncbi.nlm.nih.gov/books/NBK27156/

Jia, J., Ga, L., Liu, Y., Yang, Z., Wang, Y., Guo, X., Ma, R., Liu, R., Li, T., Tang, Z., & Wang, J. (2022). Serine protease inhibitor Kazal type 1, a potential biomarker for the early detection, targeting, and prediction of response to immune checkpoint blockade therapies in hepatocellular carcinoma. *Frontiers in Immunology, 13,* 923031. https://doi.org/10.3389/fimmu.2022.923031

Korkmaz, B., Horwitz, M. S., Jenne, D. E., & Gauthier, F. (2010). Neutrophil elastase, proteinase 3, and cathepsin G as therapeutic targets in human diseases. *Pharmacological Reviews, 62*(4), 726–759. https://doi.org/10.1124/pr.110.002733

Li, L., Peng, X., Batliwala, M., & Bouvier, M. (2023). Crystal structures of MHC class I complexes reveal the elusive intermediate conformations explored during peptide editing. *Nature Communications, 14*, 5020. https://doi.org/10.1038/s41467-023-40736-6

Peters, H. L., Tripathi, S. C., Kerros, C., Katayama, H., Garber, H. R., St John, L. S., Federico, L., Meraz, I. M., Roth, J. A., Sepesi, B., Majidi, M., Ruisaard, K., Clise-Dwyer, K., Roszik, J., Gibbons, D. L., Heymach, J. V., Swisher, S. G., Bernatchez, C., Alatrash, G., Hanash, S., … Molldrem, J. J. (2017). Serine proteases enhance immunogenic antigen presentation on lung cancer cells. *Cancer Immunology Research, 5*(4), 319–329. https://doi.org/10.1158/2326-6066.CIR-16-0141

Shklovskaya, E., & Rizos, H. (2021). MHC class I deficiency in solid tumors and therapeutic strategies to overcome it. *International Journal of Molecular Sciences, 22*(13), 6741. https://doi.org/10.3390/ijms22136741

Wang, R., Natarajan, K., & Margulies, D. H. (2009). Structural basis of the CD8 alpha beta/MHC class I interaction: Focused recognition orients CD8 beta to a T cell proximal position. *Journal of Immunology, 183*(4), 2554–2564. https://doi.org/10.4049/jimmunol.0901276

White, K. D., Gaudieri, S., & Phillips, E. J. (2014). HLA and the pharmacogenomics of drug hypersensitivity. In S. Padmanabhan (Ed.), *Handbook of pharmacogenomics and stratified medicine* (pp. 437–465). Academic Press. https://doi.org/10.1016/B978-0-12-386882-4.00021-9

Xiang, S., Yang, L., He, Y., Ding, F., Qiao, S., Su, Z., Chen, Z., Lu, A., & Li, F. (2025). Alpha-1 antitrypsin as a regulatory protease inhibitor modulating inflammation and shaping the tumor microenvironment in cancer. *Cells, 14*(2), 88. https://doi.org/10.3390/cells14020088

Zou, F., Schmon, M., Sienczyk, M., Grzywa, R., Palesch, D., Boehm, B. O., Sun, Z. L., Watts, C., Schirmbeck, R., & Burster, T. (2012). Application of a novel highly sensitive activity-based probe for detection of cathepsin G. *Analytical biochemistry*, *421*(2), 667–672. https://doi.org/10.1016/j.ab.2011.11.016

8. APPENDICES

Table A 1. Human apoptosis array coordinates and corresponding targets/controls.

Coordinate	Target/Control	Coodinate	Target/Control
A1, A2	Reference Spots	C13, C14	HO-2/HMOX2
A23, A24	Reference Spots	C15, C16	HSP27
B1, B2	Bad	C17, C18	HSP60
B3, B4	Bax	C19, C20	HSP70
B5, B6	Bcl-2	C21, C22	HTRA2/Omi
B7, B8	Bcl-x	C23, C24	Livin
B9, B10	Pro-Caspase-3	D1, D2	PON2
B11, B12	Cleaved Caspase-3	D3, D4	p21/CIP1/CDKN1A
B13, B14	Catalase	D5, D6	p27/Kip1
B15, B16	cIAP-1	D7, D8	Phospho-p53 (S15)
B17, B18	cIAP-2	D9, D10	Phospho-p53 (S46)
B19, B20	Claspin	D11, D12	Phospho-p53 (S392)
B21, B22	Clusterin	D13, D14	Phospho-Rad17 (S635)
B23, B24	Cytochrome c	D15, D16	SMAC/Diablo
C1, C2	TRAIL R1/DR4	D17, D18	Survivin
C3, C4	TRAIL R2/DR5	D19, D20	TNF RI/TNFRSF1A
C5, C6	FADD	D21, D22	XIAP
C7, C8	Fas/TNFRSF6/CD95	D23, D24	PBS (Negative Control)
C9, C10	HIF-1α	E1, E2	Reference Spots
C11, C12	HO-1/HMOX1/HSP32		